



Trans. Nonferrous Met. Soc. China 34(2024) 3412-3424

Transactions of Nonferrous Metals Society of China

www.tnmsc.cn



Enhanced dealkalization of bauxite residue through calcium-activated desulfurization gypsum

Yu-jun WU¹, Sheng-guo XUE², Li-ping LIU¹, Feng LI¹, Graeme J. MILLAR³, Fei GE¹, Jiang TIAN¹

- 1. College of Environment and Resources, Xiangtan University, Xiangtan 411105, China;
- 2. School of Metallurgy and Environment, Central South University, Changsha 410083, China;
 - 3. School of Mechanical, Medical and Process Engineering, Faculty of Engineering, Queensland University of Technology, Brisbane, Queensland 4000, Australia

Received 9 March 2024; accepted 30 August 2024

Abstract: A novel integrated approach to remove the free alkalis and stabilize solid-phase alkalinity by controlling the release of Ca from desulfurization gypsum was developed. The combination of recycled FeCl₃ solution and EDTA activated desulfurization gypsum lowered the bauxite residue pH to 7.20. Moreover, it also improved the residual Ca state, with its contribution to the total exchangeable cations increased (68%–92%). Notably, the slow release of exchangeable Ca introduced through modified desulfurization gypsum induced a phase transition of the alkaline minerals. This treatment stabilized the dealkalization effect of bauxite residue via reducing its overall acid neutralization capacity in abating pH rebound. Hence, this approach can provide guidance for effectively utilizing desulfurization gypsum to achieve stable regulation of alkalinity in bauxite residue.

Key words: bauxite residue; desulfurization gypsum; EDTA activation; alkalinity regulation; recycled FeCl₃

1 Introduction

The stacking of strongly alkaline bauxite residue not only occupies valuable land but also risks contaminating surrounding soil and ground-water with alkaline substances [1,2]. Consequently, the potential environmental problems associated with the bauxite residue disposal areas (BRDAs) have received substantial attention from both the government and the public. The content of free alkalis (NaAl(OH)₄, Na₂CO₃, etc.) directly determines the alkalinity of bauxite residue [3]. Moreover, alkaline minerals, serving as an alkali reservoir [4], are difficult to completely remove from bauxite residue, thus leading to a prevalent pH rebound during the alkalinity regulation process [5].

The alkaline components from bauxite residue are buffered in the order of acid-alkali neutralization, ion exchange, and mineral hydrolysis upon the introduction of exogenous acids [6,7]. The alkaline anions can be easily removed, but chemically bound alkalis are embedded in the residue as more stable minerals with higher content and complex compositions, necessitating enough strong acid and sufficient time for neutralization [8]. Therefore, bauxite residue neutralization is susceptible to two negative problems: (1) excessive neutralization induces high leaching of alkaline minerals; (2) the dissolution balance between alkaline solids and free alkalis is disrupted. These outlined adverse factors may also impact the stability of alkali-containing minerals.

Existing methods for alkalinity regulation

include acid/seawater neutralization, gypsum amendment, and microbial remediation [9-11]. Notably, industrial waste is of particular interest for regulating the alkalinity of bauxite residue. For example, XING et al [12] have successfully employed recycled FeCl₃ solution for this purpose. Nevertheless, flue gas desulfurization (FGD) gypsum waste is more commonly applied for remediating BRDAs due to its low cost [13–15]. The application of gypsum is complex and depends on factors such as the method of addition, dissolution rate, and the identity of alkaline anions in the residue. MENZIES and KOPITTKE [16] revealed that the combined application of seawater and gypsum can improve the availability of calcium in bauxite residue and correspondingly enhance the alkalinity reduction efficiency. Although this integrated approach is an improvement over gypsum alone, there remain problems such as long-term remediation capacity and poor reliability. These problems arise mainly from the ability of bauxite residue to effectively sequester exogenously added calcium. Gypsum can exist stably in the bauxite residue, but its lower solubility will cause a low Ca content [17]. As a result, the efficiency of gypsum to neutralize the alkalinity of bauxite residue is limited.

Solubilization of gypsum by complexation is a common method currently used [18-20]. The most reported chemical employed is EDTA which can complex with Ca²⁺ to form a chelate [Ca-EDTA] (Eq. (1)) due to the presence of four carboxyl groups [21], which leads to the gradual dissolution of calcium sulfate. Moreover, the solution pH will affect the ability of EDTA to chelate with Ca²⁺, thus forming different chelate complexes. In particular, the most negatively charged anion EDTA⁴⁻ has the strongest chelating ability, and its chelating ability is enhanced as the pH increases [22]. When the solution pH>7, the majority of EDTA exists as HEDTA³⁻ and EDTA⁴⁻, forming chelate complexes with Ca²⁺ that are difficult to release. Conversely, a decrease in pH also results in the gradual release of Ca²⁺ from these complexes. The stoichiometric ratio of Ca²⁺ bonded to EDTA is between 0.97 and 1.04 at pH 6 [23,24]. EDTA is therefore considered as a potential material for gypsum solubilization.

$$Ca^{2+}+SO_4^{2-}+EDTA^{4-}+2Na^{+}+2H^{+} \rightarrow$$
[Ca-EDTA]²⁻+2Na⁺+2H⁺+SO₄²⁻ (1)

The aim of this study is to neutralize the free

alkalis using an appropriate amount of FeCl₃, followed by the application of calcium ion activator to achieve gypsum solubilization for the stable regulation of alkaline minerals. The column experiments for the integrated application of FeCl₃ and calcium ion activator were conducted (1) to observe the phase transformation of alkaline minerals and their embedding characteristics, (2) to analyze the changes in saturation of available state of Ca in FGD gypsum and the acid neutralization behavior of bauxite residue, and (3) to clarify the stabilization mechanism of alkaline components in bauxite residue. This work will develop an economically feasible technique for Ca-driven stable regulatory of alkalinity within bauxite residue.

2 Experimental

2.1 Materials

Bauxite residue used in this study was obtained from the bauxite residue disposal areas near Henan Zhongzhou Aluminum Co., Ltd. (China). The main physicochemical properties of the bauxite residue are given in Table S1 (see Supporting Information (SI)). FGD gypsum was also provided by Zhongzhou Aluminum Co., Ltd. (China). The chemical compositions of bauxite residue and FGD gypsum were determined by X-ray fluorescence spectrometry (XRF, Table S2 in SI). Ferric chloride (FeCl₃·6H₂O) was mixed with deionized water to obtain a Fe3+ solution with a concentration of 10 g/L, which was selected to neutralize the free alkali of the bauxite residue. Activator EDTA (C₁₀H₁₆N₂O₈, analytical reagent) and CaCl₂ (analytical reagent) were purchased from Shanghai Sinopharm Chemical Reagent Ltd., China.

2.2 Experimental procedures

The leaching process of alkaline components from BRDAs was simulated by using a laboratory soil column testing unit. To reduce the difference between laboratory and field conditions, the depth of the amendment mixed layer and the amount of leaching were implemented according to the actual remediation depth of the BRDAs (80 cm) and the local rainfall (700 mm/a), respectively. The soil columns were prepared from a polymethyl methacrylate (PMMA) cylinder (height of 105 cm; inner diameter of 15 cm). Figure S1 is SI shows a

schematic diagram of the soil column leaching during bauxite residue dealkalization. Notably, the leachate collectors were placed below the soil column and the water feeder (connected to the peristaltic pump) was positioned above the column. Five soil columns were established, with a layer of nylon mesh (0.45 mm) placed at the bottom of each column, and a 15 cm layer of quartz sand placed on the porous stainless-steel partition. Five columns were filled with 20 cm of bauxite residue, and the detailed descriptions of the different treatments are given in Table 1.

Table 1 Different treatments for bauxite residue

| Group | Treatment |
|-------|---|
| CK | Column 1 was leached with deionized water |
| BGW | Column 2 was added with 3 wt.% FGD gypsum and leached with deionized water |
| BGEW | Column 3 was added with 3 wt.% of FGD gypsum and 1 wt.% of EDTA with deionized water leaching |
| BGEF | Column 4 was added with 3 wt.% of FGD gypsum and 1 wt.% of EDTA, combined with 10 g/L FeCl ₃ solution leaching |
| BC | Column 5 was leached with CaCl ₂ solution of 10 g/L |

After filling the soil column, the moistureholding capacity was calculated based on the water content in the bauxite residue. A required amount of deionized water was delivered to the individual column using a peristaltic pump. The soil column was then equilibrated for 48 h before starting the leaching experiment. During the first 38 d, leaching was conducted every two days, and the amount of leaching water was calculated as a proportion of the local average annual rainfall (1100 mm) [25], and then the soil column was monitored for 30 d once the leaching was completed. Figure S2 in SI shows the daily average temperature and humidity of the laboratory from 0 to 60 d. Following each leaching experiment, the leachates were collected, and their ion concentration, pH, and electrical conductivity (EC) were determined before the next leaching event. All treated soil columns were destructively sampled on Day 60, and then the leaching residues were washed several times with deionized water before being used for subsequent acid neutralization capacity titration experiments (ΔANC), X-ray diffraction (XRD), X-ray fluorescence spectroscopy (XRF), scanning electron microscopy-energy spectroscopy (SEM-EDS), X-ray photoelectron spectroscopy (XPS) analysis, and for determination of the physicochemical properties, including pH, EC and exchangeable sodium saturation percentage (ESP). The titration of acid neutralization capacity (ANC) of treated bauxite residue at pH 8 was determined using a long-term titration method [26] (see Section 1.1 in SI).

2.3 Sample analysis and characterization

The pH and EC values of the leachate collected during each leaching process were immediately determined by using a pH meter and a conductivity meter, while the Na and Ca contents were directly determined by inductively coupled plasma—atomic emission spectrometry (ICP—AES). The exchangeable cations (Na, Ca, Mg, and K) were determined by ammonium acetate extraction, wherein 20 mL of 1 mol/L acetic acid was employed to extract 2 g of bauxite residue. The filtered leachate was used to determine the Na, Ca, Mg and K content by ICP—AES.

The microstructure of the samples was investigated by using scanning electron microscopy (Quanta 250 FEG, FEI, USA), and the elemental distribution and content were analyzed by energy dispersive spectroscopy (INCA X-Max50, Oxford, UK). The mineral compositions of the raw and treated bauxite residue were determined by X-ray diffraction (D/max 2500v/pc, Cu Kα radiation). Ca and Fe species were analyzed using X-ray photoelectron spectroscopy (ESCALAB 250Xi, Thermo Fisher-VG Scientific Instruments Co., USA).

2.4 Statistical analysis

The SPSS 21.0 software package was used for statistical analysis and multiple linear regression analysis. The results of the experimental data were presented as mean \pm standard deviation. Statistical difference analysis of relevant parameters was performed using significance *F*-test and Duncan's multiple comparison method (P<0.05 and P<0.01). The relevant graphs were plotted with Origin 9.0.

3 Results and discussion

3.1 Effect of different treatments on bauxite residue dealkalization

Figures 1(a, b, c, d) present the effects of CK,

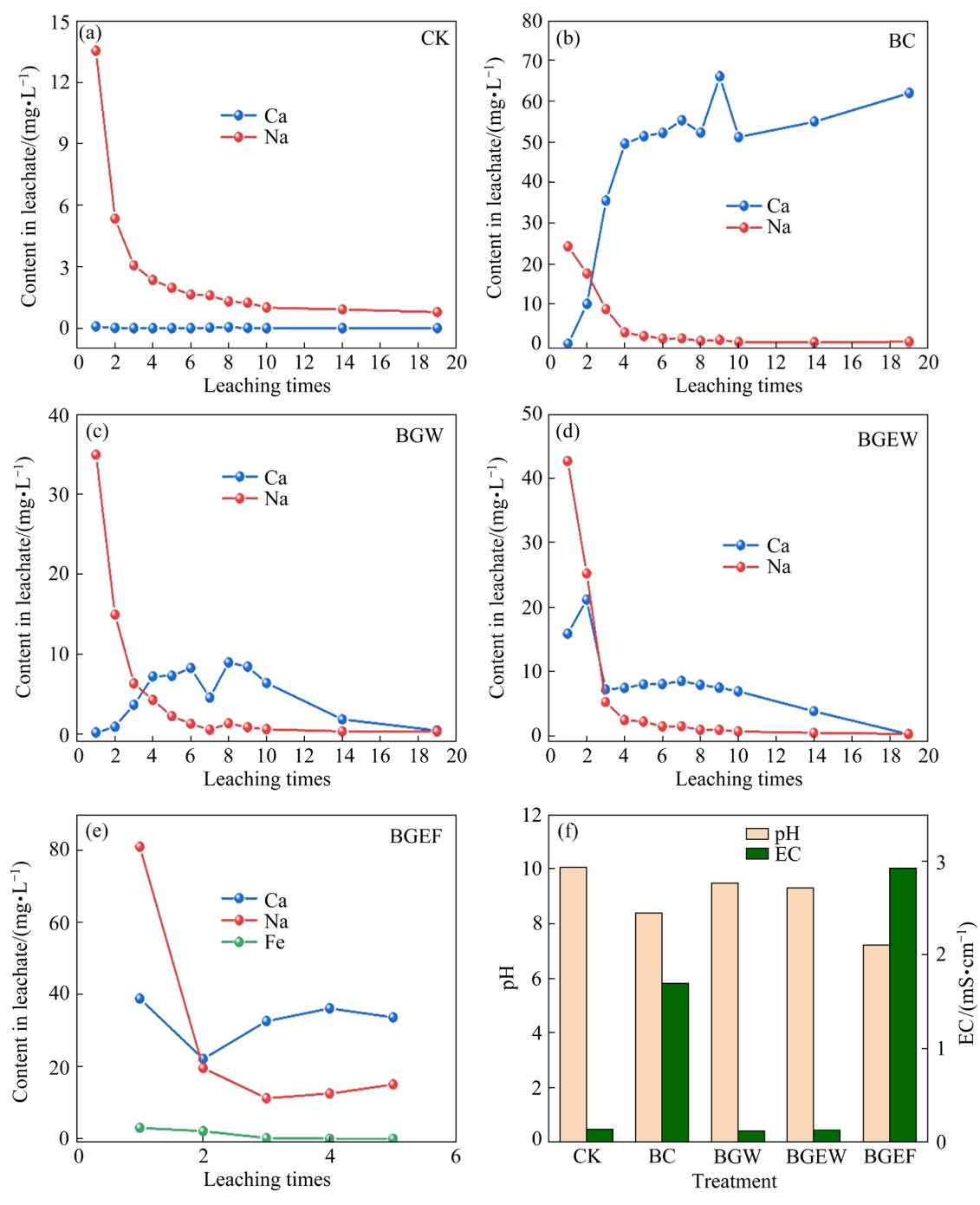


Fig. 1 Effects of different treatments on contents of Na, Ca and Fe (a-e)) in leaching solution and their effects on pH and EC (f) of bauxite residue

BC, BGW and BGEW treatments on the variation of Na and Ca contents in leachates, respectively. The leachate from CK treatment exhibited negligible presence of Ca²⁺ and the content of Na⁺ gradually decreased with increasing leaching times. However, in the leachate of BC treatment, the Na concentration also declined over time but was significantly higher than in the CK group. This situation was mainly attributed to the ion exchange

reaction between exogenous Ca²⁺ and Na⁺ sorbed on the particle surface and the replaced Na⁺ entered the leachate during the leaching process [16]. Although the trends of Na⁺ and Ca²⁺ in the BGW and BGEW treatments were similar, the solubilization effect of EDTA on the FGD gypsum resulted in higher Na⁺ and Ca²⁺ contents in the BGEW group, which led to the release of more Ca²⁺. However, the released Ca mainly presented in the

form of EDTA chelates, and their chelating ability increased with increase of pH. More importantly, the strongly alkaline environment in the bauxite residue also favored the EDTA-mediated chelation of calcium in FGD gypsum.

The Ca content in the leachate of both treatments at the late stage of leaching was close to 0, indicating that the soluble Ca present in bauxite residue was gradually leached out, and thus the leachate pH increased slowly (see Section 1.2 in SI). Both Fe and Na concentrations tended to decrease following FeCl₃ leaching, except for a slight increase observed in Ca2+ concentration after the third leaching event (Fig. 1(e)). This outlined behavior suggested that the addition of Fe³⁺ leached a greater amount of Ca²⁺ due to the consumption of alkaline anions reacting with Ca2+ through Fe3+ hydrolysis [27]. Also, the increased H⁺ aided the slow release of Ca²⁺ from the chelate complexes. Compared to the control group (pH=10.46, Fig. 1(f)), the pH of bauxite residue in the BC and BGEF treatments was 8.35 and 7.20, respectively, indicating that the BGEF treatment exhibited the best performance in regulating the alkalinity of bauxite residue.

Initially, in alkalinity regulation using calcium ions, the added EDTA may chelate with dissolved Ca from the desulfurized gypsum, entrapping Ca in the leachate to prevent its reaction with free alkali [22]. Subsequently, retained Ca is released gradually to react with alkaline minerals until the free alkalis are removed, stabilizing the dealkalization effect of bauxite residue, consistent with the ion concentration changes in the leachate. The principle of selecting Fe³⁺ to remove free alkali from bauxite residue involves two main processes: (1) the direct reaction between Fe³⁺ and soluble alkaline substances (NaOH, Na₂CO₃, and NaHCO₃, Eqs. (2)–(4)) [12]; (2) H⁺ produced by the hydrolysis of Fe3+ reacting with NaAl(OH)4 and insoluble substances (Eqs. (5) and (6)) [28]. Consequently, using FeCl₃ solution to remove free alkalis in bauxite residue is theoretically and economically feasible.

$$3OH^-+Fe^{3+}=Fe(OH)_3\downarrow$$
 (2)

$$3\text{CO}_3^{2^-} + 2\text{Fe}^{3^+} + 3\text{H}_2\text{O} = 3\text{CO}_2\uparrow + 2\text{Fe}(\text{OH})_3 \downarrow$$
 (3)

$$3HCO_3^- + Fe^{3+} = 3CO_2 \uparrow + Fe(OH)_3 \downarrow \tag{4}$$

$$Al(HO)_4^- + H^+ = Al(OH)_3 \downarrow + H_2O$$
 (5)

3.2 Effect of calcium ion activator on availability of calcium in FGD gypsum

In comparison with the CK treatment, ESP of bauxite residue was reduced in all treatments (Fig. 2(a)). This reduction was especially notable in the BC and BGEF groups where ESP reached 11.1% and 3.2%, respectively, indicating that Ca–Na ion exchange process can reach equilibrium in the presence of sufficient Ca. In turn, a significant decrease in the exchangeable Na content in the BC treatment occurred. However, the exchangeable Na content dropped to the lowest level in the BGEF treatment, which might be related to the strong ion-exchange capacity of Fe³⁺ disrupting the Ca–Na equilibrium process that released more Na⁺.

The calcium ion-exchange capacity and its mobility affect the role of Ca in regulating bauxite residue alkalinity. For example, the exchangeable Ca content varied as a function of treatment conditions compared to the CK treatment. Additionally, the exchangeable Na concentration in each treatment decreased (Fig. 2(b)), due to the addition of gypsum, especially in the BGEF treatment which was characterized by a 182% growth in the exchangeable Ca content. The quantity of exchangeable Ca in the BGEW group was higher than that in the BGW group, but lower than that in the BC group. This discrepancy mainly resulted from the fact that the gypsum solubility enhanced by the addition of EDTA was still lower than that of CaCl₂. Generally, the increase in exchangeable Ca content corresponded to a decrease in exchangeable Na content and gypsum dissolution level (≈2.7 mS/cm). The results of calcium ion exchange capacity saturation revealed that the BC, BGW, BGEW, and BGEF treatments significantly increased the contribution of Ca to total exchangeable cations (CEC) from 68% in the CK group to 92% in the BGEF group. As exchangeable Ca had a strong negative correlation with exchangeable Na, the increased exchangeable Ca content replaced more Na⁺ sorbed on the particle surface, thus reducing the ESP to improve the physicochemical properties of bauxite residue. The increased solubility of gypsum in the BGEF treatment improved the saturation of calcium ion-exchange capacity, and a larger proportion of

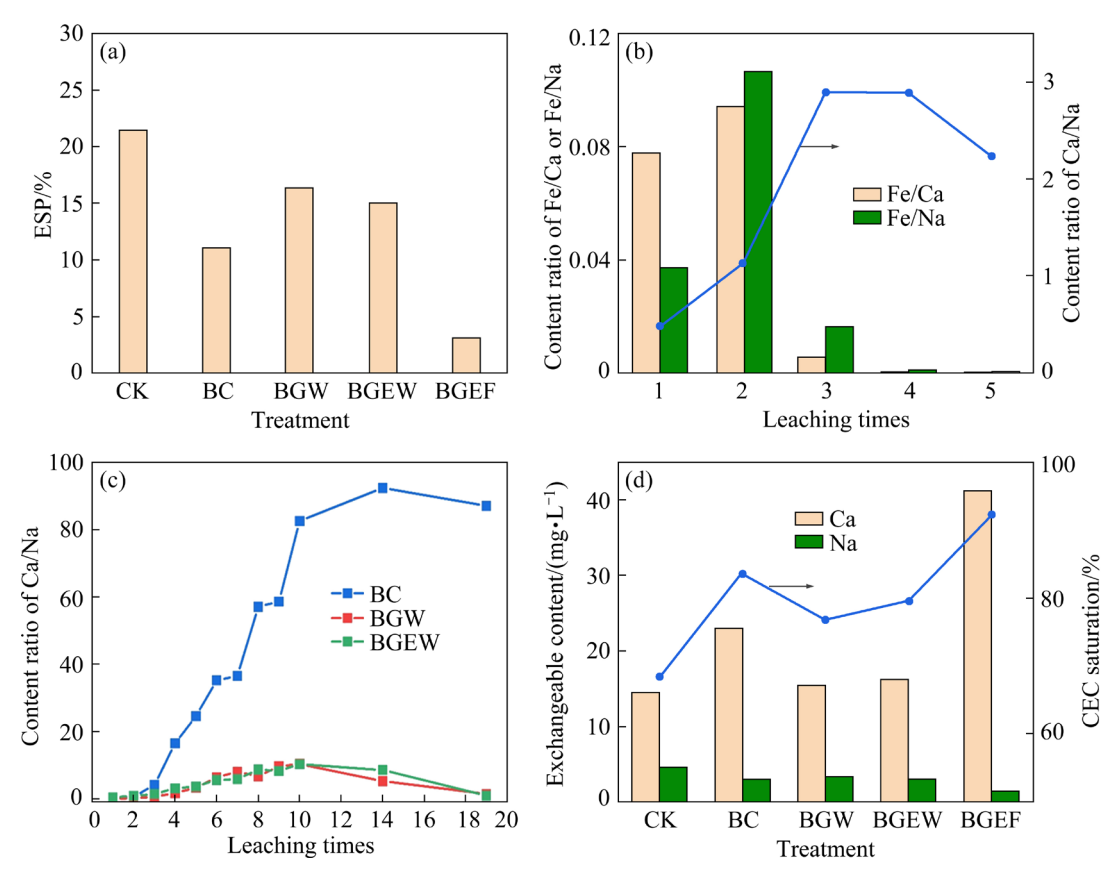


Fig. 2 Effects of different treatments on ESP for bauxite residue (a); Changes in content ratios of Ca/Na, Fe/Na, and Fe/Ca in BGEF treatment (b) and content ratios of Ca/Na in BC, BGW and BGEW treatments (c); Exchangeable contents of Na and Ca, and calcium ion exchange capacity (CEC) saturation (d) in leachates from different treatments

the released Na⁺ would exchange ions with Ca²⁺ to generate more H⁺, thus lowering the leachate pH. This behavior was consistent with the results of elevated Na and Ca in high pH leachates (Fig. 1).

The Ca/Na value (ratio of the amount of Ca consumed to Na produced) increased in the BC group as leaching time extended and then stabilized (Fig. 2(c)). This observation indicated that Ca replaced Na during the early stage of leaching. The limited solubility of FGD gypsum resulted in minimal change in Ca/Na values in the BGW and BGEW groups. Although the addition of EDTA increased the solubility of FGD gypsum, the chelation reaction between EDTA and calcium sulfate was accelerated by sodium carbonate, so that the Ca did not participate in the Ca-Na exchange reaction as shown in Eq. (7) [29]. The Fe/Na, Fe/Ca and Ca/Na values increased initially and then decreased with the increase of leaching times (Fig. 2(d)). The main reason is that after Fe³⁺ reacts with the free alkalis, the remaining Fe³⁺ undergoes ion-exchange reactions with Na and Ca. The subsequent replacement of Na by Ca resulted in a significant increase in the leachate Na content. The variation of Fe/Na was also significant due to the preferential exchange capacity of Fe for Na over Ca. Increased Fe³⁺ concentration led to significant increase in the leachate Ca2+ and Na+ concentration (Fig. 1(e)). Fe concentration remained unchanged with the depletion of exchangeable Na, which further confirmed that Fe was preferentially exchanged with Na ions. The subsequent exchange of Ca with Fe was also beneficial for bauxite residue dealkalization. Additionally, the chelation stability constant of Fe with EDTA (14.1) was greater than that of Ca (7.3), thus disturbing the chelation stability of EDTA with Ca to favor the release of Ca from the chelate complexes. This behavior was consistent with the increase in Ca content during the later stages of leaching. Hence, the Ca added as gypsum could be retained as exchangeable Ca after EDTA and gypsum application combined with FeCl₃ treatment, rather than in the form of chelate.

2CaSO₄+2Na₃HEDTA+Na₂CO₃= 2CaNaEDTA+2Na₂SO₄+H₂O+CO₂(7)

3.3 Changes in acid neutralization behavior of bauxite residue in different treatments

To study the release process of alkaline components from bauxite residue, the H⁺ addition amount (ANC) curves for different treated residues were obtained through a long-term titration process conducted over 27 d to achieve pH equilibrium at an endpoint of 8 (Fig. 3). The pH rebound occurred in all treatments apart from the BGEF group, but their ANC was significantly lower than that of the CK group. Specifically, the ANC required to achieve a titration endpoint pH of 8 for bauxite residue in the CK, BC, BGW, BGEW, and BGEF treatments were 0.5, 0, 0.2, 0.3, and 0 mmol/kg, respectively. Meanwhile, the equilibrium time to reach the titration endpoint was 14, 0, 12, 14, and 0 d, respectively. The residual pH in the BGEF group remained below 8, whereas longer equilibration time and higher acid addition were observed in other treatments during the titration process. This result implied that the bauxite residue in CK, BGW, and BGEW treatments still contained a greater amount of dissolved solid-phase alkalinity.

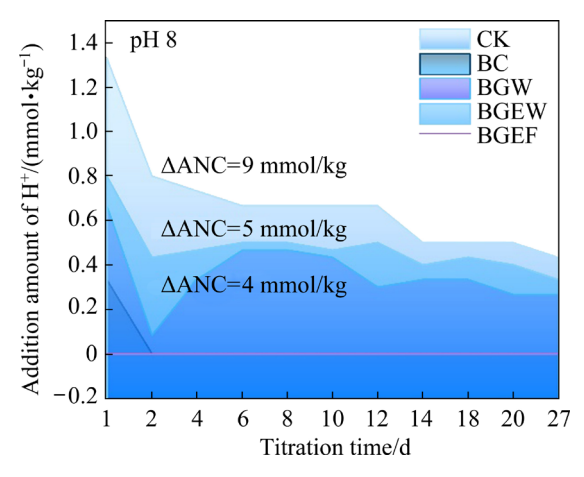


Fig. 3 Long-term titration of bauxite residue samples with pH endpoints of 8 in 27 d (Δ ANC is defined as amount of acid required to reach equilibrium of ANC curve minus the amount of initial acid added)

The slow dissolution kinetics of alkaline minerals in bauxite residue is responsible for its high pH and ANC. The Δ ANC of bauxite residue in the CK group was 0.9 mmol/kg at the end of the titration point of pH 8, while the Δ ANC of bauxite residue in the BGW and BGEW groups decreased

to 0.5 and 0.4 mmol/kg, respectively. These results indicated that the addition of FGD gypsum or its combination with EDTA reduced the ANC of residues to a certain extent. Moreover, the occurrence of milder pH rebound is primarily related to the alkaline minerals. Conventional dealkalization techniques are basically focused on the removal of free alkalis from bauxite residue, but the control of the alkalinity source is ignored, resulting in the pH rebound of treated bauxite residue. However, the application of FeCl₃ in combination with EDTA and FGD gypsum in the BGEF group can solve this problem. The EDTA increases the solubility of FGD gypsum, and the chelating ability of [Ca-EDTA] gradually weakens with decreasing pH [21]. The Ca released from the chelate complexes continues to interact with alkaline minerals after FeCl₃ solution exhausts the free alkali, thus inhibiting the dissolution process of alkaline components. Therefore, the pH of the bauxite residue in the BGEF group remained stable at 7-8, which facilitated the sustainability of the alkalinity regulation.

3.4 Mineral phase transformation in different treated bauxite residue

Compared with the CK, BC, and BGW treatments that did not significantly impact the mineral phase present, the addition of EDTA reduced the characteristic reflections of cancrinite, sodalite, calcite, and katoite in the BGEW group (Fig. 4). This observation suggests that the Ca released by the dissolution of FGD gypsum did not react directly with free alkali to form CaCO₃. Instead, a chelate was formed with EDTA, thus protecting the presence of Ca at the initial stage of alkalinity regulation. In addition, EDTA acts as a weak acid that releases H⁺ to dissolve some of the abovementioned alkaline minerals, which leads to a slight weakening of their peak intensity. For the BGEF treatment, the intensity of all phases decreased when using FeCl₃ solution to leach bauxite residue containing EDTA and detached gypsum. This process was mainly due to the strong acidic leaching solution (pH 2.5) produced by the hydrolysis of Fe³⁺ leading to the dissolution of hematite and calcite. This was consistent with the findings of KONG et al [30], who found that hematite dissolved at pH<5 when bauxite residue was treated with different acids. However, except

for hematite and calcite, the intensity of the characteristic peaks of the alkali-bearing minerals such as sodalite, cancrinite, and katoite did not decrease to a significant extent, mainly due to the Ca chelated by EDTA. The detailed information of each mineral content in the bauxite residue in different treatments is provided in Section 1.3 in SI. The weak acidic environment created by the leaching of FeCl₃ solution promotes the release of Ca from the chelate complexes. This Ca may then interact with sodalite and cancrinite without the free alkali, thus reducing their acid buffering capacity, which prevents the dissolution reaction of these two minerals.

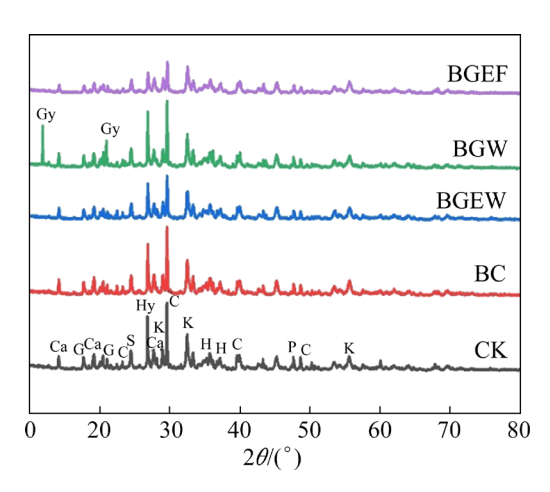


Fig. 4 XRD patterns of bauxite residue with different treatments (K-Katoite; C-Calcite; Ca-Cancrinite; H-Hematite; G-Gibbsite; Hy-Hydrogarnet; P-Perovskite; S-Sodalite; Gy-Gypsum)

3.5 Changes in surface morphology and elemental distribution of bauxite residue

There were more spherical small particles agglomerated on the particle surface in the BGEF group (detailed information of BC, BGW, and BGEW groups can be found in Section 1.4 in SI). The large agglomerates formed were more scattered and stacked together in an irregular shape, resembling the particle surface morphology in the BC group. The H⁺ incorporation leads to chemical weathering of the bauxite residue, and the small particles decomposed are further agglomerated into macroaggregates with more voids by the released Ca. The elemental distribution on the surface of bauxite residue in the BGEF group significantly different, with Na, Si, and Al changing from the previous uniform to regional distribution, and the intensity of Na signal was obviously

weakened (Fig. 5). This observation indicated that the combination of FeCl₃ and EDTA was effective in leaching Na from bauxite residue. The high content of Si, Al, and Ca, as well as a small amount of Na (10%), further demonstrated that the Ca released from the chelate entered the mineral surface or lattice by interacting with Na in cancrinite and sodalite. The distribution elemental Fe was also regional, but its signal intensity and distribution range were significantly larger. Combined with EDS analysis of Points 1, 2, 3, and 4 in the overlapping regions, the Fe contents were higher, and the Na and Ca contents were lower (<5%). Thus, it can be inferred that Fe³⁺ undergoes ion exchange with Na⁺ in alkaline minerals as well as Ca entering alkaline minerals by substitution. This deduction further proves that Fe³⁺ has a stronger exchange capacity for Na⁺ than Ca²⁺ which is in accord with the fact that higher charges are more strongly adhered to exchange sites.

3.6 Speciation transformation of Fe and Ca on mineral surfaces

The peak positions of Na 1s, Ca 2p, and Fe 2p in the XPS spectra were chemically shifted (Fig. S5 in SI), suggesting that their speciation transformed on the residue surface. The free alkalis in the BGEF group generated poorly crystallized FeOOH that was difficult to detect by XRD during the FeCl₃ neutralization process [31]. The peak fitting results of Fe 2p showed that the Fe (2p_{3/2}) and Fe (2p_{1/2}) peaks in the CK treatment appeared at (710.7±0.2) eV and (724.2±0.3) eV, respectively (Fig. 6). The addition of FeCl₃ shifted the binding energy of Fe compounds to higher values, which indicated that higher energy was required to release Fe [32,33]. Therefore, an increase in Fe—O binding resulted in a decrease in Fe activity. It has been demonstrated that the application of Fe-bearing materials increases the available content of Fe, with a relatively large proportion of amorphous Fe.

The Fe peaks $(2p_{1/2})$ in the CK, BC, BGW, and BGEW groups corresponded to β -FeOOH at 711.8 eV, while α -FeOOH was identified at 712.2 eV in the BGEF group, thus providing evidence of the transformation of goethite from β -FeOOH to α -FeOOH [34]. A slight shift in the peak position of Fe—O towards higher binding energies suggests that the application of FeCl₃ in the BGEF group brings these iron oxides into more

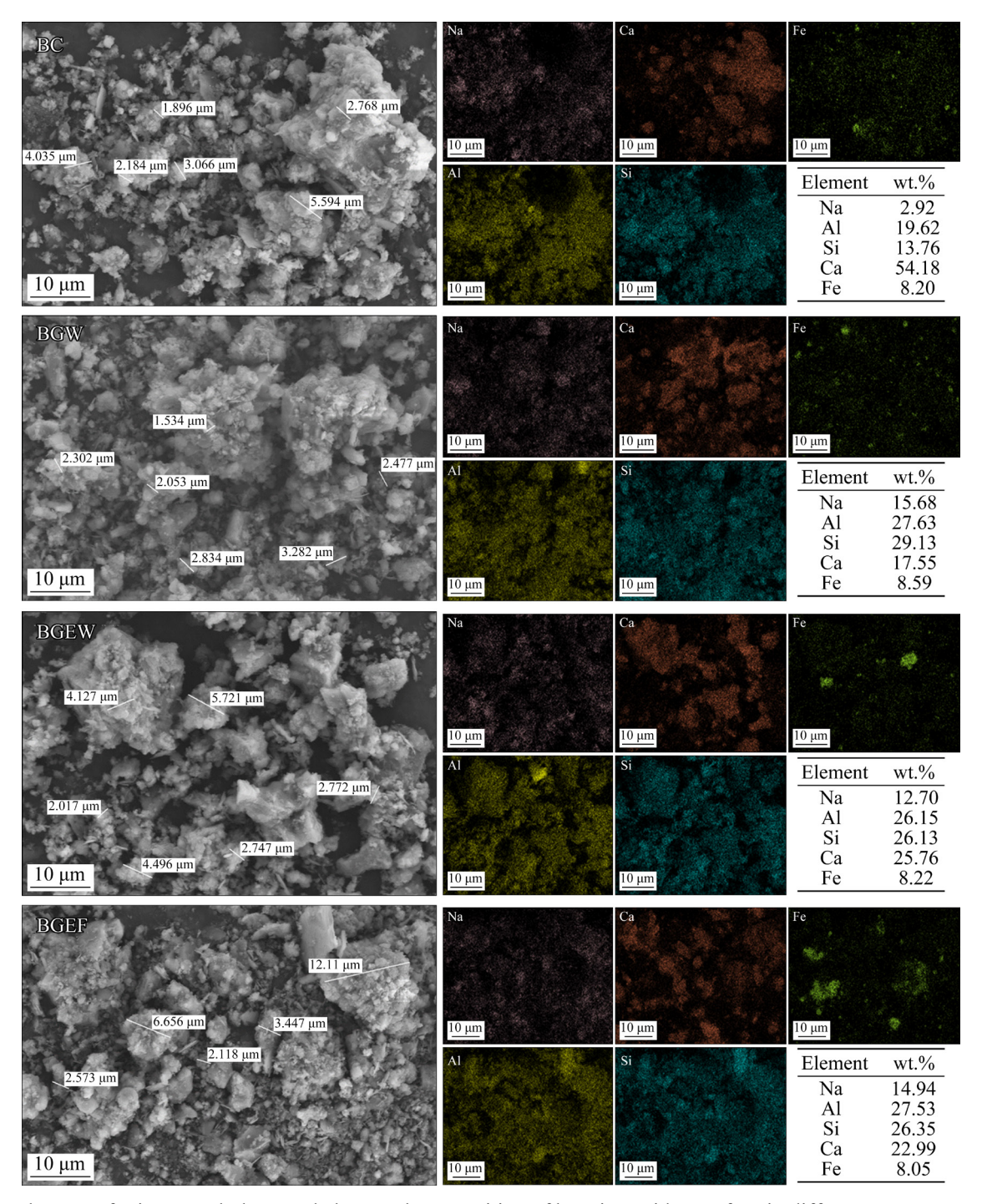


Fig. 5 Changes of micromorphology and elemental composition of bauxite residue surface in different treatments

stable states [26]. Moreover, the other stable Fe species present in each treatment was hematite. Therefore, after the exogenously added Fe neutralized the free alkalis, the increased content of Fe-containing substances primarily existed in a stable form with no secondary pollution.

Also of interest was the XPS analysis of Ca species in the various treated bauxite residue samples (Fig. 7). The two peaks of Ca 2p in the CK

group were located at 346.8 eV $(2p_{3/2})$ and 350.9 eV $(2p_{1/2})$, respectively, which were assigned to the presence of calcite [35]. After EDTA treatment, the peaks for Ca $2p_{1/2}$ and Ca $2p_{3/2}$ were shifted from 351.59–351.35 eV and 348.03–347.80 eV, respectively. Consequently, this newly generated Ca-containing component was inferred to be [Ca-EDTA] chelates [36]. Numerous studies have revealed that metal-EDTA complexes arise from

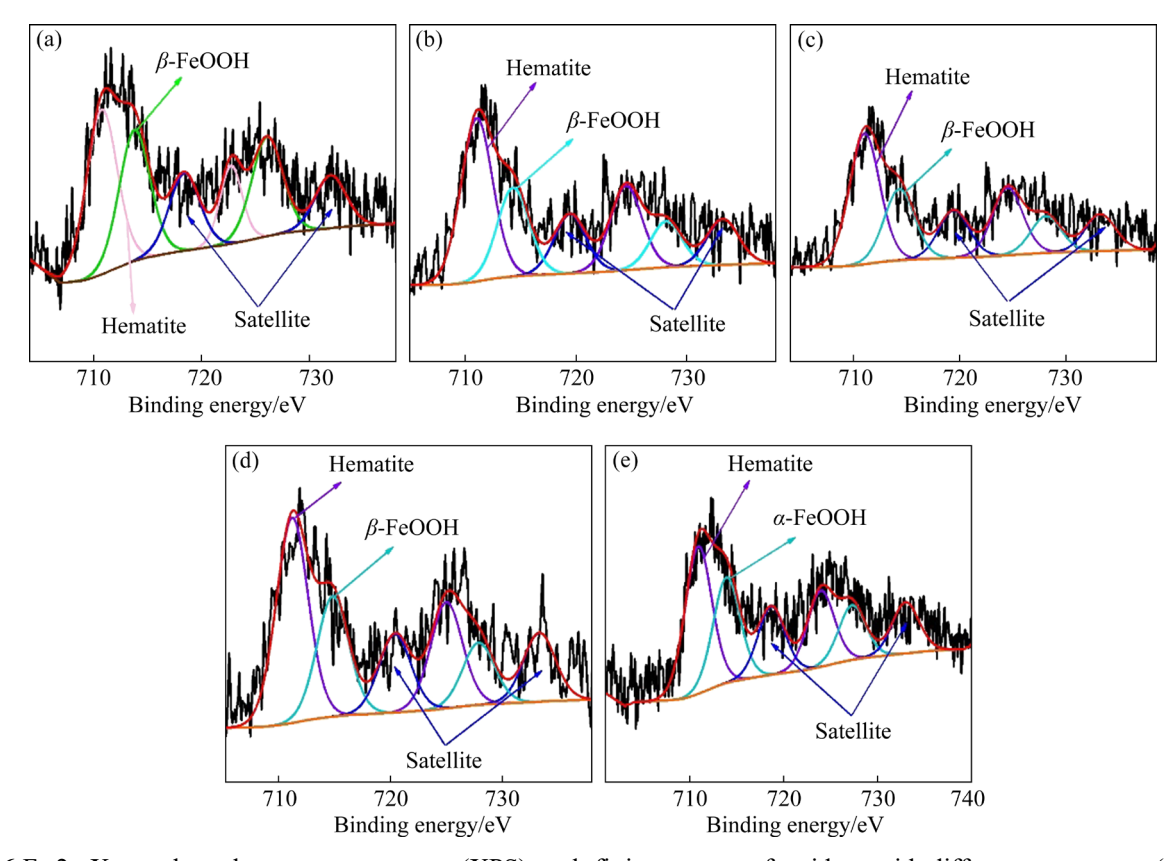


Fig. 6 Fe 2p X-ray photoelectron spectroscopy (XPS) peak-fitting spectra of residues with different treatments: (a) CK; (b) BC; (c) BGW; (d) BGEW; (e) BGEF

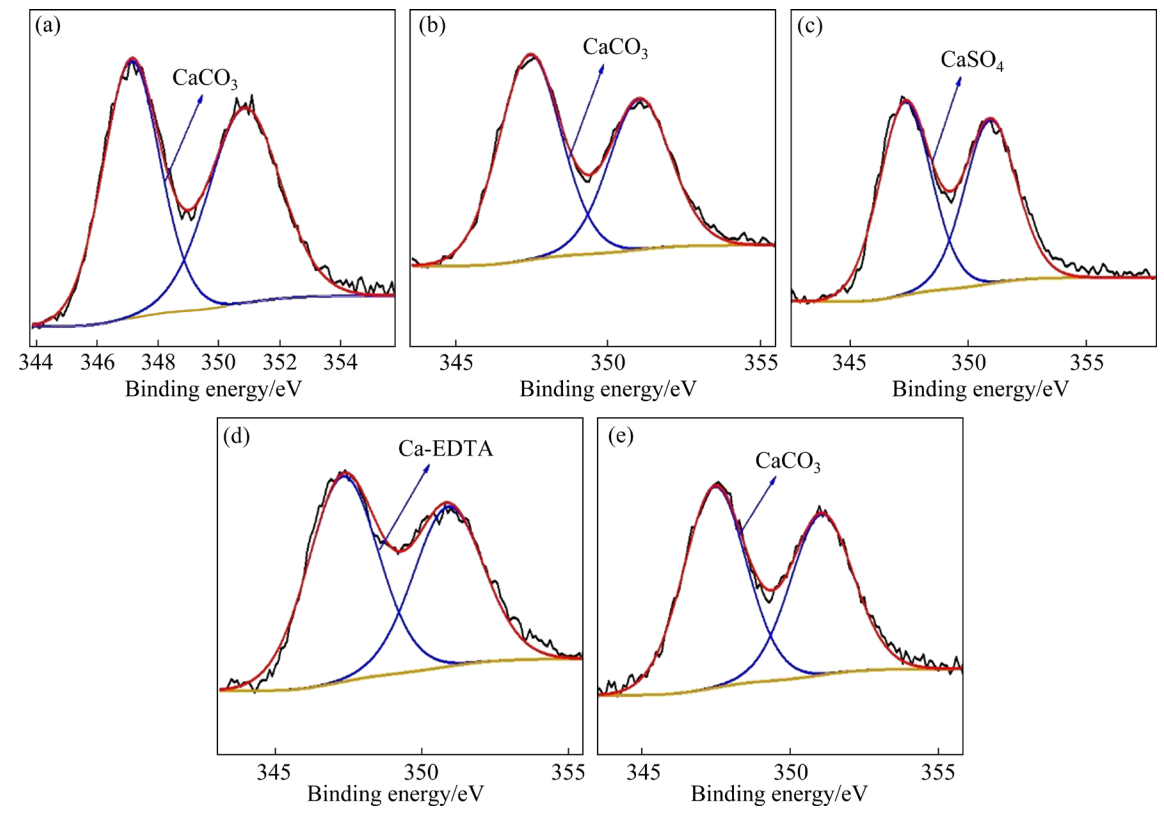


Fig. 7 Ca 2p X-ray photoelectron spectroscopy (XPS) peak-fitting spectra of residues with different treatments: (a) CK; (b) BC; (c) BGW; (d) BGEW; (e) BGEF

the complexation of nitrogen elements and carboxyl functional groups with metal elements [37]. Furthermore, the changes in binding energy (0.24 and 0.23 eV, respectively) confirmed that complexation altered the chemical environment of Ca 2p on the bauxite residue surface, with CaHCO₃⁺ and CaCO₃ (aq) being the dominant species at pH 9.0. When Ca²⁺ is mixed with EDTA, CaEDTA²⁻ is the resultant species instead of Ca²⁺ or CaCO₃(aq) [36]. The CaEDTA²⁻ chelate is more soluble in water, which favors the retention of Ca in solution rather than precipitation on the bauxite residue surface. Thus, using the chelating agent EDTA could mitigate the negative effects of alkaline anions in bauxite residue on Ca. In the BGEF group, the predominant form of Ca species was CaCO₃, consistent with the BC treatment. This was mainly attributed to the re-release of Ca from the EDTA chelate. Consequently, the presence of CaCO₃(s) in CK, BC, and BGEF treatments indicates that the production of CaCO₃(s) cannot be inhibited by the original calcite on the bauxite residue surface.

4 Conclusions

- (1) The pH of bauxite residue treated with FeCl₃ combined with EDTA and FGD gypsum (BGEF treatment) was 7.20. This strategy increased significantly the saturation of calcium ion exchange capacity in bauxite residue from 68% in the CK treatment to 92% in the BGEF treatment.
- (2) Following the combined treatment of FGD gypsum with EDTA and FeCl₃ solution, the Ca added as gypsum was retained as exchangeable calcium rather than in the form of chelates. Furthermore, the combined treatment reduced the acid neutralization capacity and pH rebound of the bauxite residue, as evidenced by the lower Δ ANC of the BGEF treatment.
- (3) The XRD, SEM-EDS and XPS analyses demonstrated the transformation and decomposition of fine-grained alkaline minerals embedded in the calcium slag after BGEF treatment. The exogenously added Fe existed in a stable state after neutralizing the free alkalis fraction in the bauxite residue, while the Ca released from the [Ca-EDTA] chelate directly stabilized the alkaline minerals.
- (4) The BGEF approach exhibited excellent performance in bauxite residue dealkalization with

notably better persistence. More importantly, the idea of alkalinity regulation with selective removal of free alkalis prior to stabilization of alkalicontaining minerals was feasible for large-scale applications.

CRediT authorship contribution statement

Yu-jun WU: Conceptualization, Methodology, Investigation, Validation, Data curation, Writing — Original draft, Writing — Review & editing; Sheng-guo XUE: Conceptualization, Methodology, Supervision, Resources, Writing — Review & editing, Project administration; Li-ping LIU: Resources, Writing — Review & editing; Feng LI: Investigation, Writing — Review & editing; Graeme J. MILLAR: Investigation, Writing — Review & editing; Fei GE: Formal analysis; Jiang TIAN: Investigation.

Declaration of competing interest

The authors declare that they have no known competing financial interests or personal relationships that could have appeared to influence the work reported in this paper.

Acknowledgments

This study was supported by the National Natural Science Foundation of China (No. 42307521), and the China Postdoctoral Science Foundation (No. 2023M742934).

Supporting Information

Supporting Information in this work can be found at: http://tnmsc.csu.edu.cn/download/22-p3412-2024-0220-Supporting Information.pdf.

References

- [1] JIANG Yi-fan, QIN Xin-feng, ZHU Feng, ZHANG Yi-fan, ZHANG Xian-chao, HARTLEY W, XUE Sheng-guo. Halving gypsum dose by Penicillium oxalicum on alkaline neutralization and microbial community reconstruction in bauxite residue [J]. Chemical Engineering Journal, 2023, 451: 139008.
- [2] WANG Chong-qing, ZHANG Xue, SUN Rui-rui, CAO Yi-jun. Neutralization of red mud using bio-acid generated by hydrothermal carbonization of waste biomass for potential soil application [J]. Journal of Cleaner Production, 2020, 271: 122525.
- [3] LI Xiao-fei, YE Yu-zhen, XUE Sheng-guo, JIANG Jun, WU Chuan, KONG Xiang-feng, HARTLEY W, LI Yi-wei. Leaching optimization and dissolution behavior of alkaline anions in bauxite residue [J]. Transactions of Nonferrous Metals society of China, 2018, 28: 1248–1255.
- [4] BRAY A W, STEWART D I, COURTNEY R, ROUT S P,

- HUMPHREYS P N, MAYES W M, BURKE I T. Sustained bauxite residue rehabilitation with gypsum and organic matter 16 years after initial treatment [J]. Environmental Science & Technology, 2018, 52: 152–161.
- [5] WU Yu-jun, JIANG Yi-fan, JIANG Jun, CHEN Li, QIN Xin-feng, HARTLEY W, XUE Sheng-guo. Conversion of alkaline characteristics of bauxite residue by mechanical activated pretreatment: Implications for its dealkalization [J]. Journal of Environmental Management, 2022, 305: 114446.
- [6] KONG Xiang-feng, GUO Ying, XUE Sheng-guo, HARTLEY W, WU Chuan, YE Yu-zhen, CHENG Qing-yu. Natural evolution of alkaline characteristics in bauxite residue [J]. Journal of Cleaner Production, 2017, 143: 224–230.
- [7] PENG Hong, KIM T, VAUGHAN J. Acid leaching of desilication products: Implications for acid neutralization of bauxite residue [J]. Industrial & Engineering Chemistry Research, 2020, 59: 8174–8182.
- [8] POWER G, GRAEFE M, KLAUBER C. Bauxite residue issues: I. Current management, disposal and storage practices [J]. Hydrometallurgy, 2011, 108: 33–45.
- [9] GUO Ying, YE Yu-zhen, ZHU Feng, XUE Rui, ZHANG Xian-chao, ZHU Ming-xing, HARTLEY W, GUO Lin, XUE Sheng-guo. Improvements on physical conditions of bauxite residue following application of organic materials [J]. Journal of Environmental Sciences, 2022, 116: 198–208.
- [10] TIAN Tao, ZHANG Chao-lan, ZHU Feng, YUAN Shan-xin, GUO Ying, XUE Sheng-guo. Effect of phosphogypsum on saline-alkalinity and aggregate stability of bauxite residue [J]. Transactions of Nonferrous Metals Society of China, 2021, 31: 1484–1495.
- [11] KONG Xiang-feng, JIANG Xing-xing, XUE Sheng-guo, HUANG Ling, HARTLEY W, WU Chuan, LI Xiao-fei. Active dealkalization of bauxite residue through integration of mechanical ball milling and flue gas desulfurization gypsum [J]. Transactions of Nonferrous Metals Society of China, 2018, 28: 534–541.
- [12] XING Yan, ZHOU Kang-gen, ZHANG Xue-kai, LEI Qing-yuan, PENG Chang-hong, SHI Yan, CHEN Wei. Application of recycled ferric chloride for alkalinity regulation of bauxite residue [J]. Journal of Cleaner Production, 2021, 305: 127174.
- [13] ZHU Feng, GUO Xu-yao, JIANG Jun, CHEN Kai-bin, ZHU Xuan-zhi, DENG Dan-dan, WU Yu-jun, HUANG Yu-wei, XUE Sheng-guo. Active dealkalization of bauxite residue through integration of mechanical ball milling and flue gas desulfurization gypsum [J]. Transactions of Nonferrous Metals Society of China, 2023. http://kns.cnki.net/kcms/detail/43.1239.TG.20231101.1648.012.html.
- [14] CARLO E D, BOULLEMANT A, COURTNEY R. Ecotoxicological risk assessment of revegetated bauxite residue: Implications for future rehabilitation programmes [J]. Science of the Total Environment, 2020, 698: 134344.
- [15] XUE Sheng-guo, ZHANG Yu-fei, JIANG Jun, LI Feng, CHEN Chao-rong, GUO Xu-yao, CHEN Qi, ZHU Feng, CHEN Hua-lin, WU Yu-jun. Effect of calcium ions on the interaction of alkaline minerals with dissolved organic matter: Implications for organic carbon sequestration in bauxite residue [J]. Plant and Soil, 2024, 497: 79–91.

- [16] MENZIES N W, KOPITTKE P M. Seawater neutralization and gypsum amelioration of bauxite refining residue to produce a plant growth medium [J]. Science of the Total Environment, 2021, 763: 143046.
- [17] WU Yu-jun, LI Xiao-fei, JIANG Jun, HARTLEY W, ZHU Feng, XUE Sheng-guo. Integrating column leaching experiments and geochemical modelling to predict the long-term alkaline stability during erosion process for gypsum amended bauxite residue [J]. Journal of Environmental Management, 2021, 289: 112479.
- [18] LEE M G, JANG Y N, RYU K W, KIM W, BANG J H. Mineral carbonation of flue gas desulfurization gypsum for CO₂ sequestration [J]. Energy, 2012, 47: 370–377.
- [19] CHANOURI H, AGAYR K, MOUNIR E, BENHIDA R, KHALESS K. Staged purification of phosphogypsum using pH-dependent separation process [J]. Environmental Science and Pollution Research, 2024, 31: 9920–9934.
- [20] GUAN Qing-jun, SUI Ying, YU Wei-jian, BU Yong-jie, ZENG Chu-xiong, LIU Chu-feng, ZHANG Zhen-yue, GAO Zhi-yong, CHI Ru-an. Moderately efficient leaching of rare earth elements from phosphogypsum via crystal regulation with EDTA-2Na during gypsum phase transformation and recovery by precipitation [J]. Hydrometallurgy, 2022, 214: 105963.
- [21] XIE Rong-quan, FENG Zu-de, LI Si-wei, XU Bin-bin. EDTA-assisted self-Assembly of fluoride-substituted hydroxyapatite coating on enamel substrate [J]. Crystal Growth & Design, 2011, 11: 5206–5214.
- [22] CHEN Hai-feng, SUN Kai, TANG Zhi-yong, LAW R V, MANSFIELD J F, CZAJKA-JAKUBOWSKA A, CLARKSON B H. Synthesis of fluorapatite nanorods and nanowires by direct precipitation from solution [J]. Crystal Growth & Design, 2006, 6: 1504.
- [23] CHRISTENSEN T, GOODEN D M, KUNG J E, TOONE E J. Additivity and the physical basis of multivalency effects: A thermodynamic investigation of the calcium EDTA interaction [J]. Journal of the American Chemical Society, 2003, 125: 7357–7366.
- [24] WU Yu-jun, DENG Dan-dan, JIANG Jun, LI Feng, ZENG Jia-qing, GUO Xu-yao, ZHU Feng, JIANG Yi-fan, XUE Sheng-guo. Ca-driven stable regulatory of alkalinity within desilication products: experimental, modeling, transformation mechanism and DFT study [J]. Science of the Total Environment, 2023, 868: 161708.
- [25] WU Yu-jun, LI Meng, FU Ding, SANTINI T C, JIANG Jun, HARTLEY W, XUE Sheng-guo. Simulation study for the formation of alkaline efflorescence on bauxite residue disposal areas following the phosphogypsum addition [J]. Journal of Cleaner Production, 2020, 262: 121266.
- [26] REN Xue-qian, ZHANG Xi, TUO Pin-peng, YANG Bin, CHEN Juan, GUO Wei, REN Jie. Neutralization of bauxite residue with high calcium content in abating pH rebound by using ferrous sulfate [J]. Environmental Science and Pollution Research, 2022, 29: 13167–13176.
- [27] BYRNE R H, LUO Y R, YOUNG R W. Iron hydrolysis and solubility revisited: Observations and comments on iron hydrolysis characterizations [J]. Marine Chemistry, 2000, 70: 23–35.
- [28] ZHANG Duo-rui, CHEN Hong-rui, NIE Zhen-yuan, XIA

- Jin-lan, LI Er-ping, FAN Xiao-lu, ZHENG Lei. Extraction of Al and rare earths (Ce, Gd, Sc, Y) from red mud by aerobic and anaerobic bi-stage bioleaching [J]. Chemical Engineering Journal, 2020, 401: 125914.
- [29] JIA Cai-yun, CHEN Qiao-shan, ZHOU Xu, WANG Hao, JIANG Guang-ming, GUAN Bao-hong. Trace NaCl and Na₂EDTA mediated synthesis of α-calcium sulfate hemihydrate in glycerol-water solution [J]. Industrial & Engineering Chemistry Research, 2016, 55: 9189–9194.
- [30] KONG Xiang-feng, LI Meng, XUE Sheng-guo, HARTLEY W, CHEN Cheng-rong, WU Chuan, LI Xiao-fei, LI Yi-wei. Acid transformation of bauxite residue: Conversion of its alkaline characteristics [J]. Journal of Hazardous Materials, 2017, 324: 382–390.
- [31] VEMPATI R K, LOEPPERT R H. Chemistry and mineralogy of Fe-containing oxides and layer silicates in relation to plant available iron [J]. Journal of Plant Nutrition, 1988, 11: 1557–1574.
- [32] HU Yong, LIANG Sha, YANG Jia-kuan, CHEN Ye, YE Nan, KE Yan, TAO Shuang-yi, XIAO Ke-ke, HU Jing-ping, HOU Hou-jie, FAN Wei, ZHU Sui-yi, ZHANG Yuan-shang, XIAO Bo. Role of Fe species in geopolymer synthesized from alkali-thermal pretreated Fe-rich Bayer red mud [J]. Construction and Building Materials, 2019, 200: 398–407.
- [33] LI Xiao-bin, ZHOU Zhao-yu, WANG Yi-lin, ZHOU

- Qiu-sheng, QI Tian-gui, LIU Gui-hua, PENG Zhi-hong. Enrichment and separation of iron minerals in gibbsitic bauxite residue based on reductive Bayer digestion [J]. Transactions of Nonferrous Metals Society of China, 2020, 30: 1980–1990.
- [34] CHEN Xing-ying, ZENG Yan-yang, CHEN Ze-hua, WANG Shuo, XIN Cheng-zhou, WANG Li-xia, SHI Chang-liang, LU Liang, ZHANG Chuan-xiang. Synthesis and electrochemical property of FeOOH/Graphene oxide composites [J]. Frontiers in Chemistry, 2020, 8: 328.
- [35] GAO Yue-sheng, GAo Zhi-yong, SUN Wei, YIN Zhi-gang, WANG Jian-jun, HU Yue-hua. Adsorption of a novel reagent scheme on scheelite and calcite causing an effective flotation separation [J]. Journal of Colloid and Interface Science, 2018, 512: 39–46.
- [36] ZHANG Wen-cai, HONAKER R Q. Flotation of monazite in the presence of calcite. Part II: Enhanced separation performance using sodium silicate and EDTA [J]. Minerals Engineering, 2018, 127: 318–328.
- [37] TIAN Jia, XU Long-hua, SUN Wei, HAN Hai-sheng, ZENG Xiao-bo, FANG Shuai, HONG Kai, HU Yue-hua. The selective flotation separation of celestite from fluorite and calcite using a novel depressant EDTA [J]. Powder Technology, 2019, 352: 62–71.

钙活化脱硫石膏强化赤泥脱碱

吴玉俊¹, 薛生国², 刘丽坪¹, 李 峰¹, Graeme J. MILLAR³, 葛 飞¹, 田 江¹

- 1. 湘潭大学 环境与资源学院,湘潭 411105;
- 2. 中南大学 冶金与环境学院,长沙 410083;
- School of Mechanical, Medical and Process Engineering, Faculty of Engineering, Queensland University of Technology, Brisbane, Queensland 4000, Australia

摘 要:提出一种通过控制脱硫石膏中钙的释放行为来去除赤泥游离碱和稳定结合碱的新方法。结果表明,利用FeCl₃结合 EDTA 活化脱硫石膏(钙离子活化剂)能够有效降低赤泥碱性(pH 值稳定在 7.20),显著提高钙离子交换容量饱和度,进而增加 Ca 对可交换阳离子总量的贡献(68%~92%)。交换性钙从改性脱硫石膏中缓慢释放后,使碱性矿物发生相转变。该方法通过降低赤泥整体酸中和能力抑制 pH 回升,最终稳定赤泥碱性调控效果,为脱硫石膏在赤泥碱性调控中的高效应用提供科学指导。

关键词:赤泥;脱硫石膏; EDTA 活化;碱性调控; FeCl3 回收液

(Edited by Bing YANG)